

# Spatially Offset Raman Spectroscopy for photon migration investigations in long bone

Kay Sowoidnich<sup>\*a,b</sup>, John H. Churchwell<sup>b</sup>, Kevin Buckley<sup>a,b</sup>, Jemma G. Kerns<sup>b,c</sup>,  
Allen E. Goodship<sup>b</sup>, Anthony W. Parker<sup>a,b</sup>, Pavel Matousek<sup>a,b</sup>

<sup>a</sup> Central Laser Facility, Research Complex at Harwell, STFC Rutherford Appleton Laboratory,  
Harwell Oxford OX11 0FA, UK

<sup>b</sup> UCL Institute of Orthopaedics and Musculoskeletal Science, Royal National Orthopaedic Hospital,  
London HA7 4LP, UK

<sup>c</sup> Lancaster Medical School, Faculty of Health and Medicine, Lancaster University, LA1 4YG, UK

## ABSTRACT

Raman Spectroscopy has become an important technique for assessing the composition of excised sections of bone, and is currently being developed as an *in vivo* tool for detecting bone disease using spatially offset Raman spectroscopy (SORS). The sampling volume of the Raman technique (and thus the amount of bone material interrogated by SORS) depends on the nature of the photon scattering in the probed tissue. Bone is a complex hierarchical material and to date little is known regarding its diffuse scattering properties which are important for the development and optimization of SORS as a diagnostic tool for characterizing bone disease *in vivo*. SORS measurements at 830 nm excitation wavelength are taken on stratified samples to determine the depth from which the Raman signal originates in bone tissue. Measurements are made using a 0.38 mm thin Teflon slice inserted in between layers of stacked 0.60 mm thin equine bone slices. The results show that larger SORS offsets were able to predominantly probe deeper layers within the sample. It could further be demonstrated that different Raman spectral signatures can be retrieved through up to 3.9 mm of overlying bone material with a 7 mm offset. Comparing the stack of bone slices with and without underlying bone tissue below the Teflon slice showed that thin sections of bone can lose appreciable numbers of photons through the unilluminated back surface. These findings have direct impact concerning potential diagnostic medical applications; for instance in the detection of bone tumor margins or areas of infected bone.

**Keywords:** Spatially offset Raman spectroscopy (SORS), photon migration, bone, diffuse scattering, sub-surface analysis, turbid medium

## 1. INTRODUCTION

Raman spectroscopy can provide chemically specific information and is therefore widely applied as an analytical tool in a number of areas. However, in its conventional form confocal Raman microscopy restricts the sample volume probed to depths of, typically, around 100-200  $\mu\text{m}$ . The advent of spatially offset Raman spectroscopy (SORS) enables to breach these limits and has proven successful in numerous applications<sup>1</sup>. The SORS technique is based on a spatial separation of the point of sample illumination by the excitation laser beam and the point at which the Raman scattered photons are collected. A small spatial offset will favor the detection of photons emerging from near the surface while larger offsets increase the chances of detecting photons from deeper layers. Near infrared excitation wavelengths facilitate higher penetration depths into the probed sample, in particular human tissue, as this spectral region exhibits low light absorption for the vast majority of (biological) samples.

The ability of SORS to extract chemical information from deep inside the sample (up to several mm) has paved the way for numerous applications in non-destructive sub-surface analysis<sup>2</sup>. Especially in the biomedical field SORS is rapidly becoming a valuable tool for tissue analysis<sup>3</sup>. Application areas include the identification of breast calcifications<sup>4</sup> and the detection of tumors<sup>5</sup>. Intensive research has also been performed on transcutaneous bone characterization to assess material composition for potential bone disease diagnosis<sup>6-8</sup>. Despite the success of SORS, a key issue remains. It is not entirely clear to what depth information is extracted for a certain spatial offset and how light scattering properties of tissues influence the SORS process at the NIR wavelengths. This paper aims to address this by carrying out investigations to gain information about photon migration inside bone.

## 2. MATERIALS AND METHODS

### 2.1 Instrumentation

The Raman investigations were performed using a custom built Raman system (Cobalt Light Systems Ltd., Oxfordshire, UK) delivering 300 mW of 830 nm radiation to the sample surface. The spatial offset was achieved by means of annular laser illumination zones with selectable radius and a fixed signal collection zone in the center of the illumination ring<sup>1</sup>. The spatial offsets between excitation and collection areas ranged from 0 mm to 7 mm. The scattered Raman radiation from the collection zone was focused into a low-loss Optran WF fiber bundle (CeramOptec, East Longmeadow, MA) and transferred into a spectrograph (Raman Explorer, Headwall, MA) equipped with a CCD detector (Andor iDus 420 BR-DD; Andor, Belfast, Northern Ireland).

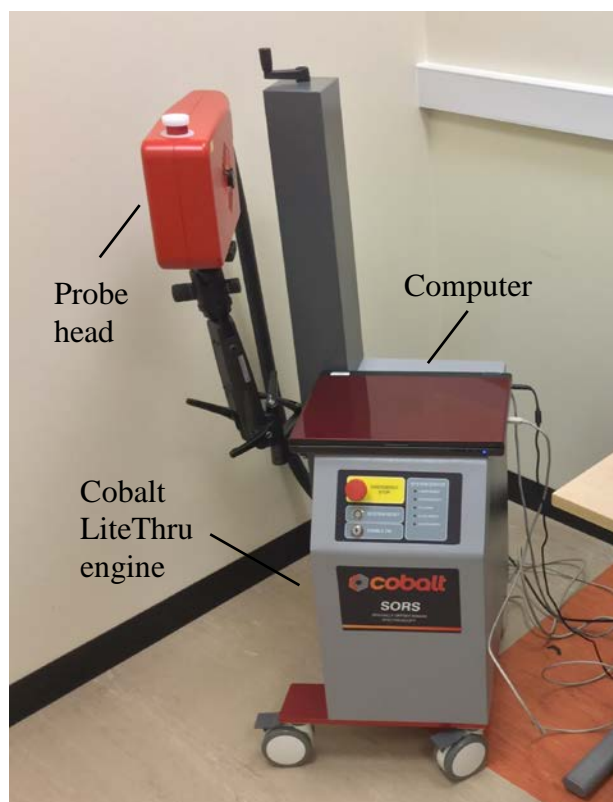


Figure 1. Photograph of the applied custom built SORS system.

### 2.2 Sample material

Tissue samples comprised section cuts from the mid-shaft as well as the end-shaft of a horse metacarpal, 4 cm in length each. By means of a bandsaw 6 slices 0.60 mm thick were cut along the long axis of the bone section. The top section was not used in the measurements due to its small size and curvature. For the photon migration studies the remaining five bone slices were stacked together in the same order they originally had within the bone before cutting, forming a stack of 4 bone-bone interfaces between layers. For SORS measurements a slice of Teflon (polytetrafluoroethylene) with a thickness of 0.38 mm was inserted between individual bone layers within the stack, and below the stack. For each Teflon depth position three lateral positions were probed and at each spot 200 spectra with an integration time of 0.1 s were collected. To investigate a possible influence of an additional bone volume below the stack of bone slices experiments were repeated with the corresponding bone segments below the stack of bone slices. Raman intensity ratios were determined considering the most prominent bands of Teflon at  $733\text{ cm}^{-1}$  as well as bone at  $961\text{ cm}^{-1}$ .

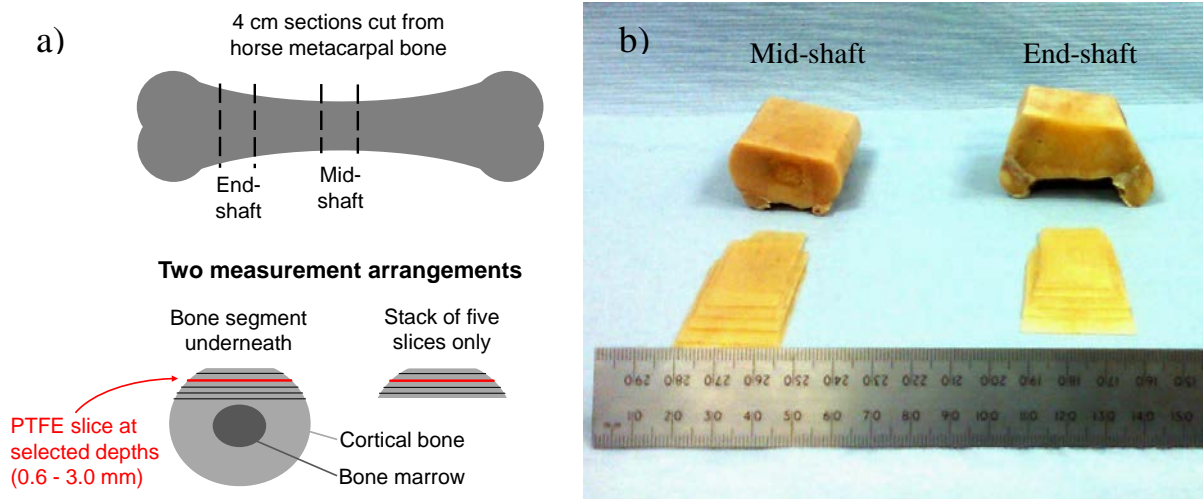


Figure 2. Schematic representation of used bone sample and measurement arrangements (a), photograph of cut sections and slices from the mid-shaft as well as from the end-shaft (b).

### 3. RESULTS AND DISCUSSION

#### 3.1 SORS spectra of buried Teflon layer

Teflon was selected as it has a strong single band at  $733\text{ cm}^{-1}$  which is in the vicinity but completely resolved from the strong bone phosphate signal at  $961\text{ cm}^{-1}$ . The material thickness of  $0.38\text{ mm}$  was selected to achieve band intensity in the same order of magnitude as the bone phosphate band. Figure 3 displays Raman spectra for SORS offsets of  $0\text{ mm}$ ,  $2\text{ mm}$ ,  $4\text{ mm}$ , and  $6\text{ mm}$  when the Teflon layer is located below  $3\text{ mm}$  of horse metacarpal end-shaft and with the bone segment placed below the stack of slices. For clarity the broad background due to fluorescence interference was removed by subtracting a 5<sup>th</sup> order polynomial from each spectrum<sup>9</sup>. When the Teflon layer was measured through  $3\text{ mm}$  of bone material the prominent Teflon band at  $733\text{ cm}^{-1}$  was still observable in the spectra.

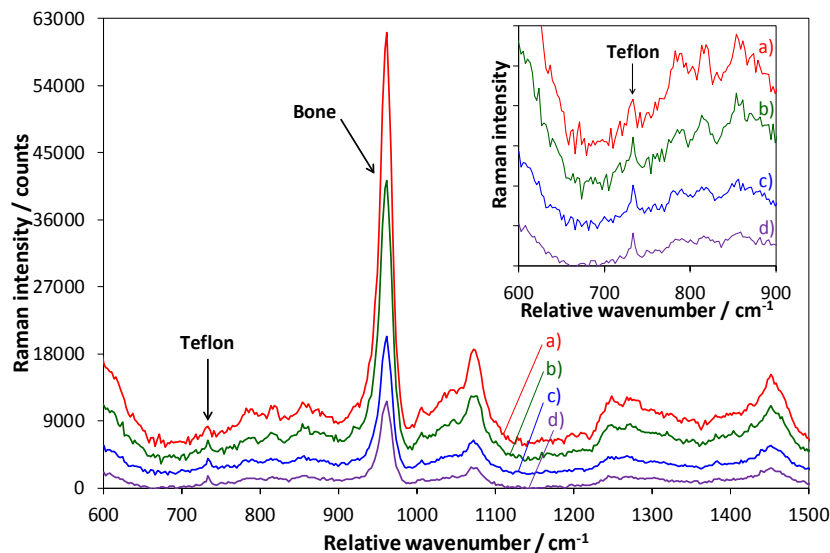


Figure 3. Background-corrected Raman spectra of horse metacarpal end-shaft with a Teflon layer located below  $3\text{ mm}$  of bone and above the bone segment shown for selected SORS offsets, a)  $0\text{ mm}$ , b)  $2\text{ mm}$ , c)  $4\text{ mm}$ , d)  $6\text{ mm}$ , spectra are shifted vertically for clarity, insert depicts expanded view of the Teflon Raman band.

In Figure 4, the Teflon to bone intensity ratio and the signal-to-noise (S/N) ratio of the Teflon band at  $733\text{ cm}^{-1}$  are presented as a function of the applied SORS offset. Although the absolute intensities were slightly higher for small spatial offsets the Teflon to bone ratio increased from about 1.7 % for zero offset to 8.1 % for a SORS offset of 7 mm. A similar trend can be observed for the S/N ratio of the most intense Teflon band with values increasing from 2.7 at 0 mm offset up to about 7.8 at offsets greater than 6 mm. Both graphs demonstrate a superior visibility of the small Teflon signal using large SORS offsets due to a combination of increased Teflon to bone ratio and larger S/N ratios.

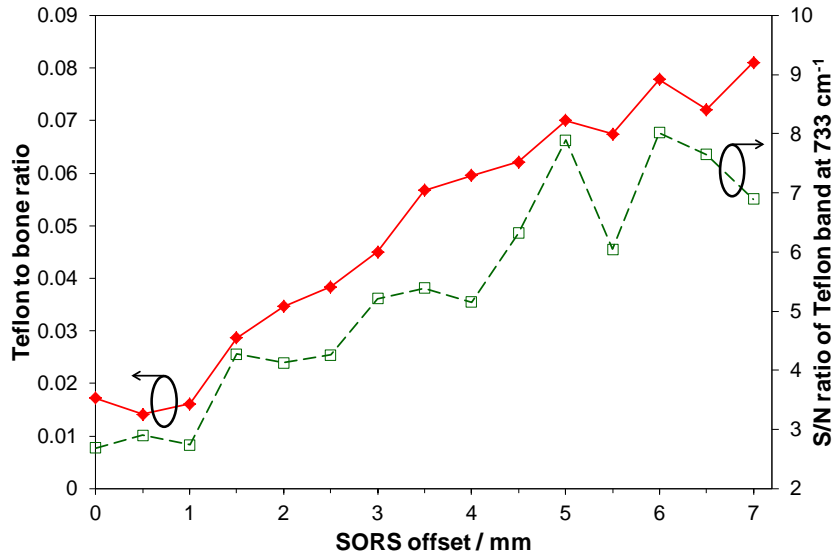


Figure 4. Teflon to bone intensity ratios (left-hand scale) and S/N ratios of the Teflon band at  $733\text{ cm}^{-1}$  (right-hand scale) in dependence from SORS offset, Teflon layer located below 3 mm of horse metacarpal end-shaft bone with the bone segment in place beneath the Teflon slice.

When investigating the Teflon below the 5 bone slices, without solid bone material underneath, the same trend can be observed albeit with the Teflon to bone ratios reduced by up to 52 % and the S/N ratios of the Teflon band reduced by up to 58 %. These dramatic reductions are ascribed to the missing bone material underneath. Without a diffusely scattering medium underneath photons passing through the Teflon slice retain their propagation direction and therefore cannot contribute to the Raman signal intensity. In contrast, with the bone underneath the Teflon laser photons (as well as) which have already travelled through the thin Teflon sample have a certain probability to reverse their propagation direction by means of multiple diffuse scattering inside the underlying bone. This diffuse scattering can partly be regarded as a “photon reversal” redirecting at least some photons back towards the overlaying Teflon. Hence, these additional laser photons can undergo Raman scattering inside the Teflon hereby increasing the Raman signal intensity.

The Teflon to bone intensity ratios were calculated for all investigated SORS offsets and selected data are displayed in Figure 5 as a function of the overlaying bone thickness above the Teflon slice. The decrease in the intensity ratio is much more pronounced for small SORS offsets than for large offsets. The overall reduction going from 0.6 mm depth to 3 mm depth amounts to 94 % and 67 % for SORS offsets of 0 mm and 6 mm, respectively. This can be explained as smaller offsets will give a higher ratio for smaller depths as the Teflon volume and the probed volume have a maximum overlap in that case. Moving the Teflon deeper inside the bone will reduce the spatial overlap and hence the Teflon to bone ratio resulting in the observed dramatic decrease. In contrast, using a 6 mm spatial offset, i.e. probing greater depths, results in a small ratio when the Teflon sample is located at a small depth. Here, increasing the Teflon depth inside the bone will consequently increase the overlap with the sampled volume leading to larger values for the Teflon to bone ratio. However, in all cases this effect is accompanied by an overall signal decrease with increasing depth leading to the observed curve shapes.

### 3.2 Dependence of signal recovery with depth from SORS offset

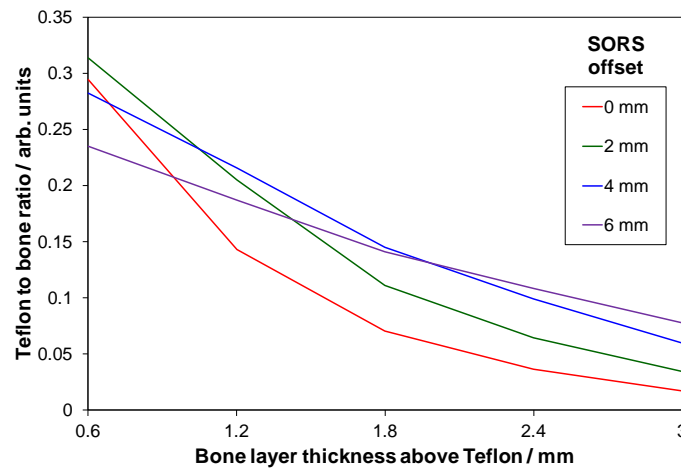


Figure 5. Teflon to bone ratios dependence on bone layer thickness above the Teflon slice using bone slices of horse metacarpal end-shaft with the bone segment located underneath the stack of slices.

From the data also the SORS offset giving the maximum Teflon to bone intensity ratio for a given Teflon depth within the bone layer stack has been determined. The resulting plots in figure 6 give valuable information about the approximate depth from which the main signal contribution arises when a specific spatial offset is applied. If the bone segment is in place beneath the slices there is a monotonic increase in SORS offset required to retrieve the maximum signal contribution with increasing depth. As an example, to interrogate the sample predominantly at a depth of 3 mm requires SORS offsets of 8 mm and 7 mm for mid-shaft bone and end-shaft bone, respectively. In contrast, when using the slices only, the spatial offset necessary to obtain the maximal Teflon to bone intensity ratio exhibits only small variation when the Teflon slice is moved to depths larger than about 1.8 mm. At that point, already significant amounts of photons get lost through the unilluminated back-surface of the bone layer stack. However, at lower Teflon depths inside the bone there is still a sufficient amount of bone material below the Teflon layer to enable effective backscattering of photons resulting in similar curve shapes for using the slices with and without the bone segment underneath it.

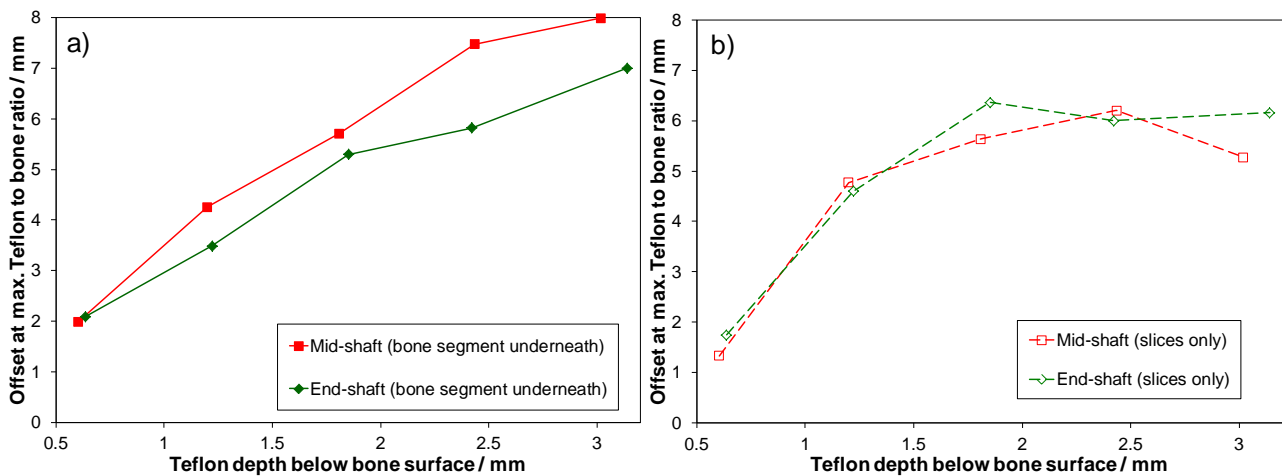


Figure 6. SORS offsets required to obtain maximum Teflon to bone intensity ratio for selected Teflon depths below the bone surface for horse metacarpal mid-shaft and end-shaft, slices with bone segment underneath in place (a), stack of five bone slices only (b).

### 3.3 Maximum accessible penetration depth for signal recovery

Based on the 3-sigma criterion and taking into account the S/N ratios of the Teflon band at  $733\text{ cm}^{-1}$  penetration depths for a given SORS offset were estimated. It is noteworthy that even for zero spatial offset depths of 2.8-3.0 mm can be probed in the applied illumination and collection configuration. This is particularly advantageous when investigating biological samples as probing a larger volume helps to reduce inhomogeneities. When having the bone segment in place underneath the stack of 5 bone slices penetration depths of up to 3.7 mm and 3.9 mm can be realized using 7 mm spatial offset for mid-shaft bone and end-shaft bone, respectively. Considering the bone slices only, i.e. without a diffusely scattering medium underneath penetration depths are generally lower. The reduction was ca. 4-6 % for small offsets and increased up to 22 % for large SORS offsets due to the missing “photon reversal” effect.

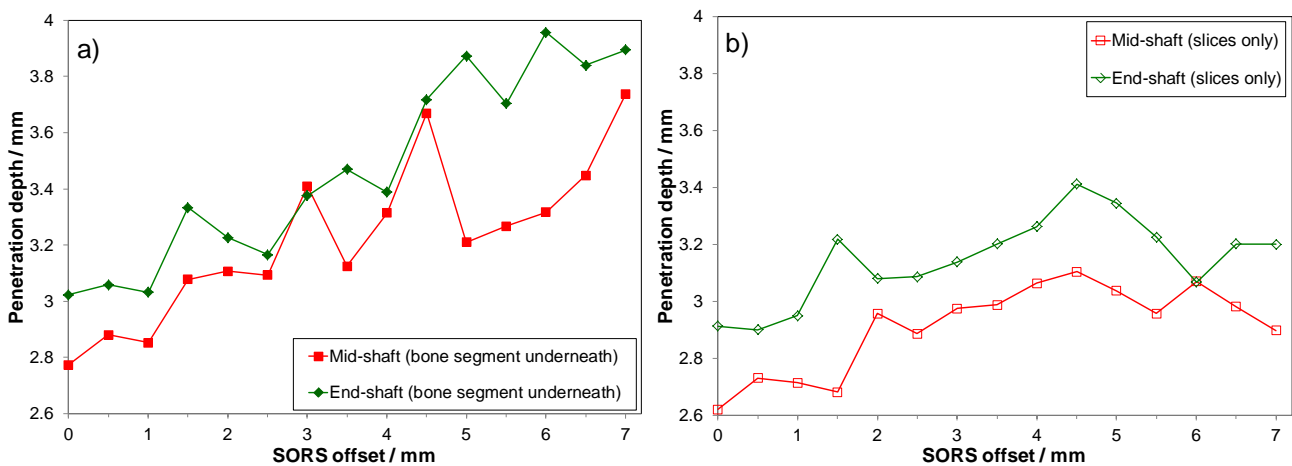


Figure 7. Estimated penetration depths dependent from applied SORS offset based on the 3-sigma criterion for horse metacarpal mid-shaft and end-shaft, slices with bone segment underneath in place (a), stack of bone slices only (b)

## 4. CONCLUSION

The research undertaken provides valuable information about photon migration inside selected bone material. For a given SORS offset the approximate location of the probed volume within the bone material, i.e. at what depth Raman signals are predominantly detected from, has been determined. To enable effective signal recovery from the desired depth it is essential that a sufficiently large amount of diffuse scattering material is present beneath that depth within the sample. When this condition is met and using Teflon as an example, a novel type of signal arising from a substance chemically different from and not present in the native bone spectrum could be recovered through up to 3.9 mm of compact bone tissue. These findings have a direct impact for medical diagnostics using SORS, e.g. enabling the non-invasive detection of spectral changes caused by cancer or infection deep inside the bone.

## ACKNOWLEDGEMENTS

The authors wish to thank the Engineering and Physical Sciences Research Council (EP/H002693/1), the Science and Technology Facilities Council, and University College London for their support.

## REFERENCES

- [1] Matousek, P., "Inverse Spatially Offset Raman Spectroscopy for Deep Noninvasive Probing of Turbid Media," *Appl. Spectrosc.* 60(11), 1341-1347 (2006).
- [2] Buckley, K. and Matousek, P., "Non-invasive analysis of turbid samples using deep Raman spectroscopy," *Analyst* 136(15), 3039-3050 (2011).
- [3] Matousek, P. and Stone, N., "Recent advances in the development of Raman spectroscopy for deep non-invasive medical diagnosis," *J. Biophotonics* 6(1), 7-19 (2013).
- [4] Stone, N., Baker, R., Rogers, K., Parker, A. W. and Matousek, P., "Subsurface probing of calcifications with spatially offset Raman spectroscopy (SORS): future possibilities for the diagnosis of breast cancer," *Analyst* 132(9), 899-905 (2007).
- [5] Keller, M. D., Vargis, E., de Matos Granja, N., Wilson, R. H., Mycek, M.-A., Kelley, M. C. and Mahadevan-Jansen, A., "Development of a spatially offset Raman spectroscopy probe for breast tumor surgical margin evaluation," *J. Biomed. Opt.* 16(7), 077006-1-077006-8 (2011).
- [6] Schulmerich, M. V., Dooley, K. A., Vanasse, T. M., Goldstein, S. A. and Morris, M. D., "Subsurface and Transcutaneous Raman Spectroscopy and Mapping Using Concentric Illumination Rings and Collection with a Circular Fiber-Optic Array," *Appl. Spectrosc.* 61(7), 671-678 (2007).
- [7] Okagbare, P. I., Begun, D., Tecklenburg, M., Awonusi, A., Goldstein, S. A. and Morris, M. D., "Noninvasive Raman spectroscopy of rat tibiae: approach to *in vivo* assessment of bone quality," *J. Biomed. Opt.* 17(9), 090502-1-090502-3 (2012).
- [8] Buckley, K., Kerns, J. G., Gikas, P. D., Birch, H. L., Vinton, J., Keen, R., Parker, A. W., Matousek, P. and Goodship, A. E., "Measurement of abnormal bone composition *in vivo* using noninvasive Raman spectroscopy," *IBMS BoneKEy* 11, Article number 602 (2014).
- [9] Lieber, C. A. and Mahadevan-Jansen, A., "Automated Method for Subtraction of Fluorescence from Biological Raman Spectra," *Appl. Spectrosc.* 57(11), 1363-1367 (2003).